Local structure in the paraelectric phase of $Cd_2Nb_2O_7$ determined from x-ray diffuse scattering, by means of *ab initio* molecular dynamics and Monte Carlo modeling

Marek Paściak,* Marek Wołcyrz, and Adam Pietraszko
Institute of Low Temperature and Structure Research, Polish Academy of Sciences, P.O. Box 1410, 50-950 Wrocław, Poland

Stefano Leoni†
Max-Planck-Institut für Chemische Physik fester Stoffe, Nöthnitzer Str. 40, D-01187 Dresden, Germany
(Received 14 August 2009; published 13 January 2010)

X-ray diffuse scattering in the paraelectric phase of $Cd_2Nb_2O_7$ is measured and structurally interpreted using atomistic methods. *Ab initio* molecular-dynamics simulations show dynamic disorder in both sublattices with average displacements of Cd ions significantly larger than for Nb. Within octahedral NbO_6 and zigzag CdO chains along ⟨110⟩ rather strong longitudinal correlations of ion displacements are found whereas the transverse component is weakly correlated. Local distortions lead to shifts of valence bond sums for cations toward nominal values. In combination with Monte Carlo simulations, excellent agreement of calculated and experimental diffuse scattering patterns is achieved.

DOI: 10.1103/PhysRevB.81.014107 PACS number(s): 77.80.−e, 61.43.Bn, 61.05.cf, 77.84.Ek

I. INTRODUCTION

$Cd_2Nb_2O_7$ (CNO) has recently been of special interest due to its peculiar ferroelectric behavior. On lowering temperature it is known to undergo several phase transitions;[1,2] among them a transition with broad heat-capacity anomaly[3] and frequency-dependent change in dielectric constant[1,4,5] has been observed at about 196 K. The explanation of the latter is still controversial. Some authors suggest a polydispersive relaxation mechanism[6] whereas others attribute it to the paraelectric to ferroelectric "diffuse" phase transition[7] which qualifies the compound as a relaxor ferroelectric. However, unlike other relaxors (e.g., Pb-based perovskites[8,9]), CNO does not contain any kind of chemical disorder and therefore the concept of random field cannot be applied here. Most of the studies underline the role of dynamic disorder of Cd atoms, the so-called hopping mode that couples to the ferroelectric soft mode.[3,4,10]

The structure of the high-temperature paraelectric phase of CNO, existing above 205 K, was determined by several authors.[11–13] Paraelectric CNO is cubic ($a \simeq 10.4$ Å) and crystallizes in the pyrochlore-type structure with $Fd\bar{3}m$ space group (Fig. 1). The structure can be viewed as composed of two interpenetrating sublattices: (i) a network of corner-sharing NbO_6 octahedra (the oxygen atoms building octahedra are hereafter labeled O2) and (ii) a network of O1-Cd-O1 zigzag chains, which occupy the empty spaces between the octahedra.

Despite many studies, the structures of the numerous low-temperature phases of CNO remain largely obscure, mainly due to severe crystal twinning making routine structure analysis very difficult. The only experimental paper by Weller *et al.*[13] reported the tetragonal structure below 180 K (with very small distortion, $c/a \approx 1.0005$). However, the space group assigned, $I\bar{4}m2$, does not permit ferroelectricity and the actual structure must be more complicated, for example, it may contain domains of lower symmetry.[13] Recently, Fischer *et al.*[14] based on *ab initio* calculation proposed structures of two subsequent low-temperature ferroelectric phases: orthorhombic *Ima*2 and monoclinic *Cc*. However, their computational approach excluded the possibility of disorder.

CNO in its paraelectric phase, as many other relaxors, shows relatively strong x-ray diffuse scattering (DS), which is caused by local symmetry breaking and short-range to medium-range correlations. Its two-dimensional character and transverse polarization (Fig. 2) suggests linear correlation within the displacive disorder (i.e., existence of chains with correlated shifts of ions). Planes of DS are oriented perpendicularly to $\langle 110 \rangle^*$ directions[16] indicating ⟨110⟩ as the direct-space directions of correlations.[17] Due to the presence of additional modulation of DS planes, the distribution of the intensities changes from uniform streaks on $hk(2n-1)$ layers to broad spots on $hk2n$ layers. Similar shape of DS was recently reported for the other pyrochlore compounds.[18]

In the present paper we report on the determination of local structure in paraelectric CNO, i.e., on the character, range, and place of occurrence of the correlations of ionic displacements. DS can provide valuable information on local two-body correlations, which is not accessible by standard crystallographic methods. However, its interpretation is never obvious and usually some joint studies are needed. Therefore we performed *ab initio* Born-Oppenheimer molecular-dynamics (MD) simulations in order to find an appropriate model for the disorder and additional correlations taking place in CNO. On the basis of MD results we constructed a simple nearest-neighbors vector model, which permits to perform Monte Carlo (MC) simulations on a larger scale. MC is nowadays the most common tool for the analysis of DS patterns.[19,20] It enables the precise calculation of DS and direct comparison with the experimental images. By means of MC local structure features extracted from *ab initio* MD simulations can be expressed on the suitable lengthscales for comparison with experiment.

II. EXPERIMENT

Single crystals of CNO were grown by the flux method using CdO as a solvent. Good quality crystals of spherical

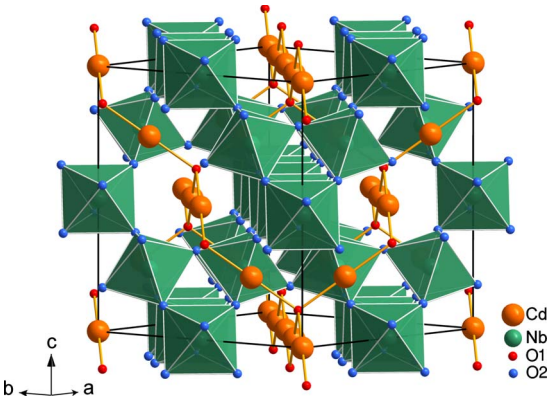

FIG. 1. (Color online) Average structure of paraelectric $Cd_2Nb_2O_7$ comprises two sublattices, both containing the atomic chains that run along ⟨110⟩ directions. Differentiation between O1 and O2 explained in the text.

shape (0.2 mm in diameter) were used for x-ray diffraction experiments. X-ray data collection was performed at room temperature (293 K) on Oxford Diffraction X'Calibur four-circle single-crystal diffractometer equipped with charge coupled device camera using graphite-monochromatized Mo Kα radiation ($\lambda = 0.71073$ Å) generated at 50 kV and 25 mA. For the determination of the average crystal structure the three-dimensional sets of x-ray diffraction data were collected in 1200 frames in the 2θ range of $3° - 93°$ with $\omega = 1.2°$ and recording time of a single frame of 35 s. Diffuse scattering data were collected only in ω-rotation mode around the [001], [010], and [110] directions with the recording time 50–90 s. The average structure of CNO was determined from 7812 collected reflections in order to control the crystal identity and quality. The structure fully overlaps the one determined by Łukaszewicz *et al.*[12] Reciprocal planes were extracted for the analysis of DS from the set of registered frames with the help of CRYSALIS software.[21] The final layer images were averaged over nine adjacent slices with a thickness covering 8% of the lattice parameter; e.g., the *hk*0.5 layer was prepared as an average of *hk*0.46 and *hk*0.54 layers.

III. RESULTS AND DISCUSSION

A. Molecular-dynamics simulations

Born-Oppenheimer *ab initio* molecular-dynamics simulations at 300 K were performed using the SIESTA code.[22] The parametrization of Perdew-Burke-Ernzerhof[23] of the exchange-correlation functional was used, together with norm-conserving Trouiller-Martins pseudopotentials. A double-ξ basis set with polarization functions was used on all atoms. To explore departure from the average symmetry, a large enough system had to be taken into account to achieve a reliable sampling. As a compromise between size and the efficiency of calculations, we have chosen an anisotropic shape of the simulated system, consisting of $4 \times 4 \times 1$ unit cells (1408 atoms). This choice is further justified by the fact that we observe experimentally $\{110\}^*$ planes of diffuse scattering. Therefore one-dimensional correlation effects confined to the *ab* crystal plane should be adequately treated in the anisotropic simulation box. We calculated a set of trajectories at 300 K propagated from different starting structures, some representing trial arrangements with correlated displacement of atoms, others being fully ordered. After equilibration, all of them quickly converged to the state of dynamic disorder described below.

The first stage of our analysis consisted of a symmetry check performed by means of KPLOT.[24] Each trajectory was time averaged over 1 ps after equilibration. Over this time scale the structures show the average space group $Fd\bar{3}m$ determined in experiment. In the second stage diffuse scattering patterns were calculated. From the set of trajectories we selected a representative one, which provided a data set consisting of 300 subsequent snapshots collected over 2 ps. To ensure good statistics of atomic pairs, DS patterns were calculated as time averages over those 300 consecutive structures. An example of DS on *hk*0.5 layer is shown in Fig. 3. Even though the distribution of intensities is rather coarse, one can easily extract the features that are characteristic for both calculated and experimental patterns. DS is transverse polarized and displays streaks perpendicular to $\langle 110 \rangle^*$ directions. Examination of adjacent reciprocal sections reveals the two-dimensional character of DS (streaks are the intersections of $\{110\}^*$ planes and *hk*0.5 layer). From the good agreement of the experimental and calculated DS patterns it can

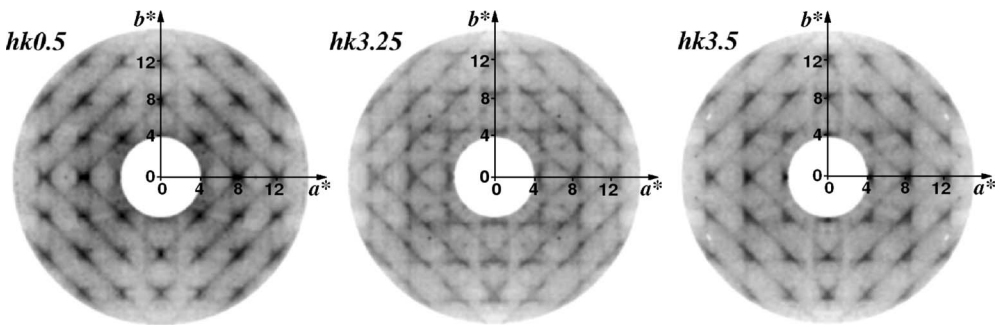

FIG. 2. Three layers of reciprocal space with nonintegral *l* displaying strong, structured diffuse scattering in the form of streaks (intersections of DS planes and the planes of the images) that run along $\langle 110 \rangle^*$ directions. Note the strong modulation of the streaks. The measurement of DS is described in Sec. II. The existence of such DS effects was recently reported by Malcherek (Ref. 15).

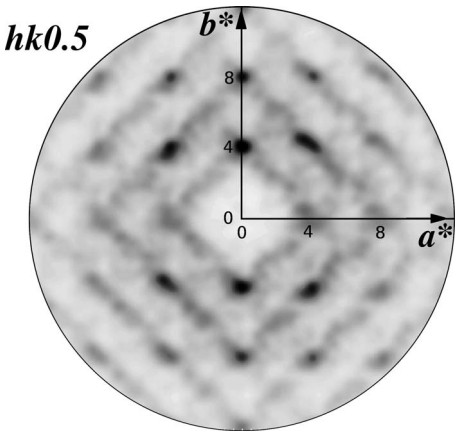

FIG. 3. Diffraction pattern of the *hk*0.5 section of reciprocal space calculated for the structures extracted from one *ab initio* MD trajectory. Its form clearly corresponds to the experimental DS pattern (cf. Fig. 2). The pattern (as well as those in Fig. 7) was calculated and displayed using DIFFUSE software (Ref. 25).

be deduced that within the simulation box there are additional correlations of displaced atoms that have to reflect the correlations in the real material. Thus, the sampling of correlated ionic displacements provided by *ab initio* MD is relevant for the analysis of disordering patterns present in the structure of CNO.

Careful examination of simulated structures excludes any static disorder as no deviation from cubic symmetry remains unchanged in time. In order to analyze the dynamic distortions that may result in the appearance of DS, we calculated two-dimensional pair-distribution function (PDF) for all the -Nb-O2- and -Cd-O1-atomic chains running parallel to *ab* plane [Figs. 4(a) and 4(b)]. PDF is defined here as

$$P(\mathbf{r}) = \frac{1}{N_A N_B} \sum_{i,j}^{N_A N_B} \delta(\mathbf{r} - \mathbf{r}_{ij}), \tag{1}$$

where N_A and N_B are the numbers of atoms of type A and B, respectively. The sum runs over all pairs of atoms in the same chain. The same set of data (300 sample structures within 2 ps time frame) as in the case of DS patterns calculation was used here. The maps of PDF (histograms on the *ab* plane) for NbO_6 and CdO sublattices are presented in Figs. 4(c) and 4(d), respectively.

The anisotropy of distribution of interatomic vectors for nearest-neighbor pairs can be clearly observed in both sublattices. However, it is definitely more pronounced within the NbO_6 sublattice [especially in the case of Nb-O2 pairs, Fig. 4(c)]. Therein, an elongated, ellipsoidal distribution is confined not only to nearest neighbors but is also characteristic of more distant atomic pairs. This anisotropy allows identification of distinct correlation directions: longitudinal and transverse with respect to the interatomic vectors and, consequently, to the atomic chains running along ⟨110⟩ directions. Transverse correlation is characterized by a rather broad PDF component compared to the longitudinal one. In order to check whether the PDF shape for Nb-O2 pairs (i.e.,

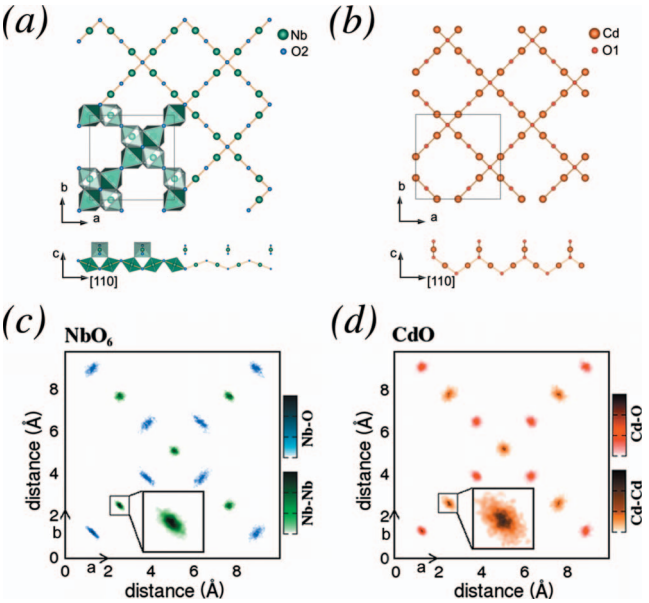

FIG. 4. (Color) A plot of Nb-O2 (a) and Cd-O1 (b) atomic chains running parallel to the *ab* plane. Two layers are extracted, each containing parallel chains that run along $[\bar{1}10]$ or [110] direction (upper and lower layer, respectively). Two-dimensional pair-distribution functions calculated for the -Nb-O2- (c) and -Cd-O1- (d) chains running parallel to *ab*, respectively. Darker colors denote larger value of $P(\mathbf{r})$—cf. Eq. (1).

the disorder in the transverse direction) may be the result of any octahedral tilting, the correlation of shifts from the average positions for *trans*-O2 atoms was checked. Since it amounts to zero (within statistical error) the transverse O2 displacements remain uncorrelated and there is no tilting. At the same time the Nb-O2 bond-length distribution is rather narrow (Fig. 5).

In the case of -Cd-O1- chains the anisotropy of PDF is weaker. Cd-Cd interatomic vector map is characterized by smeared distribution [cf. inset of Fig. 4(d)], which reflects the dynamic disorder (Cd-hopping mode) being significantly

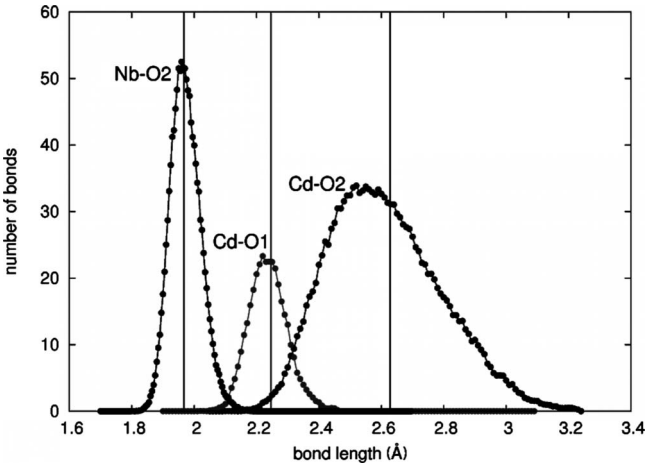

FIG. 5. Bond-lengths distribution for: Cd-O1, Cd-O2, and Nb-O2 pairs. Solid vertical lines give the average structure values (Ref. 7).

bigger than for the NbO_6 sublattice. As evidenced by the displacement parameters calculated in the directions parallel ($U^{\parallel}_{Cd}$=0.007 Å^2) and perpendicular ($U^{\perp}_{Cd}$=0.019 Å^2) to the Cd-O1 bonding, Cd atoms tend to displace in the latter direction in agreement with x-ray results.[12] For comparison, the displacement parameter for Nb is isotropic and equal to 0.014 Å^2. Similar anisotropy to that displayed by Cd was also observed for other pyrochlore compounds. In $La_2Zr_2O_7$ lanthanum atoms never occupy the exact 16*d* positions but are dynamically disordered around an annulus perpendicular to the O1-La-O1 direction.[26] The disorder of Cd together with transverse shifts of O2 atoms lead to a broad distribution of the Cd-O2 bond length (Fig. 5).

The disordered schemes evidenced by the PDF maps can be understood in terms of bond valences.[27] For the undistorted cubic structure of CNO (Ref. 12) and the pair parameters taken from Ref. 28, the valence bond sums (VBS) are: 1.6745 for Cd and 5.1982 for Nb. It is expected that strongly underbonded Cd atoms will be rather prone to leave the center of the oxygen cage in order to increase their valences. On the other hand, the only way to simultaneously lower the valence of Nb and increase that of Cd is to displace the O2 atoms in the transverse direction with respect to Nb-O2 chains. At the same time Cd atoms displace toward a given area of higher coordination by O2. The observed dynamic disorder leads to the fluctuation of valences; for Nb the average VBS is lowered to 5.02 and for Cd VBS is raised to 1.75. Thus, the dynamic structure shifts toward nominal valences.

The movement of one O2 distorts two octahedra leaving some space for transverse shift of neighboring Nb atoms. This point appears as a key issue for dielectric (relaxor) properties of CNO. Displacive disorder of O2 can be the medium for the coupling of the Cd-hopping mode and the soft mode of the NbO_6 sublattice leading to strong anharmonicity of the latter observed in many previous works.[11] Qualitatively similar disorder geometry of the two sublattices suggests already the existence of the coupling between them.

The displacement schemes resulting from *ab initio* MD are comparable only to a limited extent to the concerted shifts of atoms leading to the low-temperature phase (*Ima*2) calculated by Fischer *et al.*[14] Therein, the main ingredient of distortion responsible for the appearance of ferroelectricity is the move of Nb atoms toward the octahedral edges, i.e., rather in the longitudinal than in the transverse direction. On the other hand, the distortion of the CdO network is similar in our simulation as well as in Ref. 14: the Cd-O1 bonds remain practically unchanged and Cd atoms shift toward O2 leading to the broad distribution of Cd-O2 distances. To shed more light on the change in the dynamic disorder across the phase transitions, temperature-dependent experiments need to be performed.

B. Monte Carlo simulations

It was already shown that the local structure evidenced by *ab initio* MD produces DS patterns matching the experiment. However the size of the system affects the Fourier transform calculation and the details of DS remain unresolved. The aim of the following part of our work is to describe—on the basis of MD results—the local structure of CNO in terms of a simple, effective interaction model. Such a model enables MC simulation to be performed for a large system, and, consequently, allows for a precise calculation of DS. Since the experiment was done with x-rays, we assume that disorder of oxygens remains, according to the drastic differences in atomic scattering factors, largely invisible such that only cations have to be taken into account in the modeling.

The most important features of structural disorder evidenced by MD are the following: both sublattices are disordered, displacements within the Cd-O1 network are substantially bigger though; there is a pronounced anisotropy in the interatomic vector distribution—longitudinal components are rather close to the average-structure values, whereas there is some amount of disorder in the transverse direction. The Hamiltonian of the model taking into account these features has the form

$$H = \sum_{\langle i,j\rangle^{\langle 110\rangle}} [k_1(\Delta d^{\parallel}_{ij})^2 + k_2(\Delta d^{\perp}_{ij})^2], \tag{2}$$

where the sum runs over all nearest-neighbor pairs of cations (all in $\langle 110\rangle$ directions), $\Delta d^{\parallel}_{ij}$ is the longitudinal component of deviation from the average-structure interatomic vector, $\Delta d^{\perp}_{ij}$ gives its transverse component, and k_1 and k_2 are the coupling constants. Since the PDF maps are—as far as only cations are concerned—qualitatively the same for both sublattices, the same model can be applied for both, only the coupling constants differ. In this basic model any deviation from the average configuration of atoms costs extra energy. According to MD simulation, $k_1 > k_2$; i.e., the longitudinal coupling is much stronger. The values of atomic shifts were probed within a range consistent with *ab initio* MD (cf. mean-square displacements in Sec. I). The space of parameters k_1 and k_2 was scanned in search of the values leading to similar PDF diagrams as those presented in Figs. 4(c) and 4(d). The main factors to be compared here were the full width at half maximum values for the distribution of nearest-neighbor Nb-Nb and Cd-Cd vectors. Each simulation consisted of independent runs for the two sublattices with ca. 10^5 Monte Carlo steps. The simulation box consisted of $20 \times 20 \times 20$ unit cells and the Metropolis scheme was used for the sampling.[29] The best fit was obtained for $k_1 = 3.45\ kT$ and $k_2 = 0.75\ kT$ for Nb ions and $k_1 = 2.02\ kT$ and $k_2 = 0.43\ kT$ for Cd, respectively.

Simulation results are presented in Figs. 6 and 7. At first glance it is rather difficult to see any prominent correlations within the configuration of displacements for one layer of Nb chains (Fig. 6). However, the longitudinal components of displacements, even if rather small, are highly correlated within a given chain. The diffuse scattering pattern calculated from the simulated structure is in excellent agreement with experimental results even for high indices layers (Fig. 7), which probes the adequacy of the model applied. All elements of the patterns are reproduced—there are all equivalent $\{110\}^*$ planes visible with the characteristic modulation of the intensity. The existence of planes caused by one-dimensional, longitudinal correlations is evident.

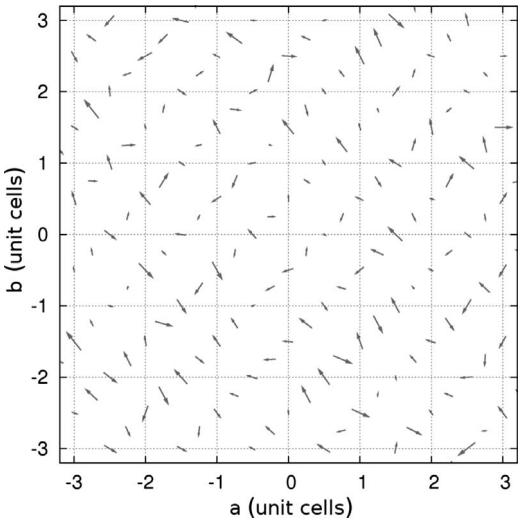

FIG. 6. Result of MC simulation: a fragment of *ab* section with the displacements for the set of Nb ⟨110⟩-oriented chains (cf. Fig. 4). Arrows denote the projections of displacements onto *ab* plane. Shifts are magnified ten times for clarity.

The modulation deserves a separate comment. Usually such effects are related to the internal structure of the objects responsible for DS (in our case ⟨110⟩-oriented atomic chains).[17] Additional simulations with different parameters of the model showed that the degree of modulation is proportional to the value of k_2. When the latter is increased with respect to the value of kT, there is an overall tendency for the system to order. Therefore, the modulation may be the measure of the interchain correlation. This issue can be properly addressed with the study of DS as a function of temperature in the context of the phase transitions occurring in CNO.

IV. CONCLUSIONS

We presented a joint experimental and theoretical study of local structure in the paraelectric phase of $Cd_2Nb_2O_7$. *Ab initio* molecular dynamics revealed dynamic disorder in both sublattices and anisotropy within the correlation of ionic displacements from an average positions. Oxygen octahedra are deformed in a way that allows the bond valence sum of Nb atoms to decrease with a simultaneous increase for the otherwise underbonded Cd atoms. Disorder of NbO_6-sublattice oxygens results in transverse (with respect to the ⟨110⟩ atomic chains) displacements of Nb atoms. As confirmed by Monte Carlo simulation, transverse disorder and longitudinal correlation of displacements of cations give rise to the characteristically structured diffuse scattering patterns, which give excellent agreement with the experimental results. From the methodological point of view we presented here a comprehensive scheme for the interpretation and simulation of diffuse scattering patterns. In our approach the modeling of disorder is based on *ab initio* molecular dynamic calculations, which are providing correlations from the true dynamics of the system, thus avoiding speculation on the origins of

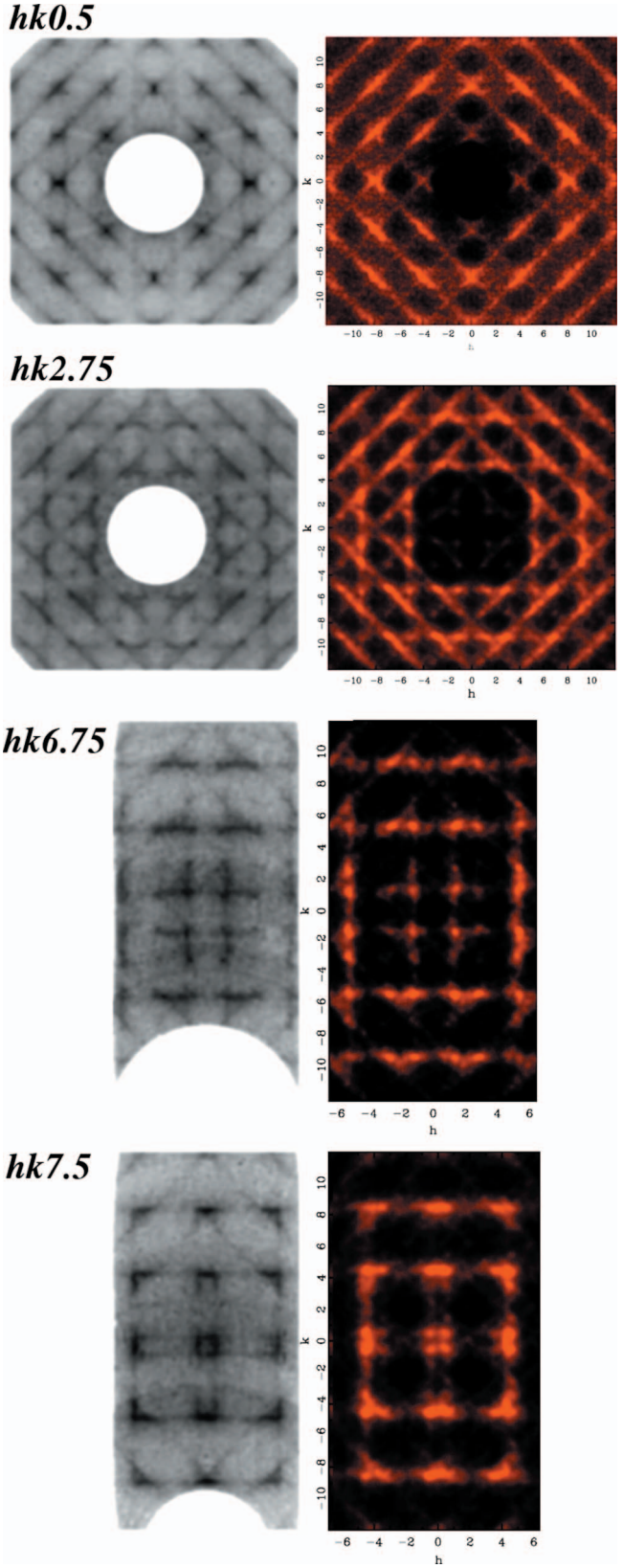

FIG. 7. (Color) Diffuse scattering on selected planes in the reciprocal space. Experimental results (left side) are compared with patterns calculated for the configurations resulting from MC simulations.

disorder. As such, our scheme translates the time evolution of displacements within a smaller system, accessible at the highest level of theory, into space distribution of correlations, which can be sampled with Monte Carlo for a larger, representative system, which allows for comparison with experiments. We believe that our scheme is general and that it can be applied to any compound displaying dynamical disorder effects.

ACKNOWLEDGMENTS

M.P. acknowledges the support from the Polish Ministry of Science and Higher Education (Grant No. N202 023334) and the IMPRS in Dresden (through the Klaus Tschira Foundation). Computational time at ZIH, Dresden and RZG, Garching is gratefully acknowledged. We would like to thank A. P. Heerdegen for the critical reading of the manuscript.

*Present address: Research School of Chemistry, Australian National University, Canberra, ACT 0200, Australia; marek.pasciak@anu.edu.au

†leoni@cpfs.mpg.de

[1] V. A. Isupov, Phys. Solid State **47**, 2119 (2005).

[2] E. Buixaderas, S. Kamba, J. Petzelt, M. Savinov, and N. N. Kolpakova, Eur. Phys. J. B **19**, 9 (2001).

[3] M. Tachibana, H. Kawaji, and T. Atake, Phys. Rev. B **70**, 064103 (2004).

[4] N. N. Kolpakova, P. Czarnecki, W. Nawrocik, M. P. Shcheglov, and L. Szczepańska, Ferroelectrics **302**, 233 (2004).

[5] C. Ang and Z. Yu, Phys. Rev. B **70**, 134103 (2004).

[6] C. Ang, R. Guo, A. S. Bhalla, and L. E. Cross, J. Appl. Phys. **87**, 7452 (2000).

[7] N. N. Kolpakova, P. P. Syrnikov, A. O. Lebedev, P. Czarnecki, W. Nawrocik, C. Perrot, and L. Szczepanska, J. Appl. Phys. **90**, 6332 (2001).

[8] G. A. Smolenskii and A. I. Agranovskaya, Phys. Solid State **1**, 1429 (1959).

[9] L. E. Cross, Ferroelectrics **76**, 241 (1987).

[10] H. Taniguchi, T. Shimizu, H. Kawaji, T. Atake, M. Itoh, and M. Tachibana, Phys. Rev. B **77**, 224104 (2008).

[11] F. Brisse, D. J. Stewart, V. Seidl, and O. Knop, Can. J. Chem. **50**, 3648 (1972).

[12] K. Łukaszewicz, A. Pietraszko, J. Stepień-Damm, and N. N. Kolpakova, Mater. Res. Bull. **29**, 987 (1994).

[13] M. T. Weller, R. W. Hughes, J. Rooke, C. S. Knee, and J. Reading, Dalton Trans. **2**, 3032 (2004).

[14] M. Fischer, T. Malcherek, U. Bismayer, P. Blaha, and K. Schwarz, Phys. Rev. B **78**, 014108 (2008).

[15] T. Malcherek, J. Phys.: Condens. Matter **19**, 275208 (2007).

[16] Note that $\langle uvw \rangle$ stands for a set of all symmetrically equivalent lattice directions $[uvw]$ both in direct and in reciprocal space, in the latter case marked with *; similarly, $\{hkl\}$ stands for a set of all symmetrically equivalent lattice planes (hkl).

[17] A. Guinier, *X-Ray Diffraction: In Crystals, Imperfect Crystals, and Amorphous Bodies* (Freeman, San Francisco, 1963).

[18] B. Nguyen, Y. Liu, and R. L. Withers, J. Solid State Chem. **180**, 549 (2007).

[19] T. R. Welberry and B. D. Butler, J. Appl. Crystallogr. **27**, 205 (1994).

[20] T. R. Welberry, *Diffuse X-Ray Scattering and Models of Disorder*, IUCr Monographs in Crystallography (Oxford University Press, Oxford, 2004).

[21] CRYSALIS *software*, Oxford Diffraction Ltd. (2009).

[22] J. M. Soler, E. Artacho, J. D. Gale, A. Garcia, J. Junquera, P. Ordejon, and D. Sanchez-Portal, J. Phys.: Condens. Matter **14**, 2745 (2002).

[23] J. P. Perdew, K. Burke, and M. Ernzerhof, Phys. Rev. Lett. **77**, 3865 (1996).

[24] R. Hundt, J. C. Schön, A. Hanneman, and M. Jansen, J. Appl. Crystallogr. **32**, 413 (1999).

[25] T. Proffen and R. B. Neder, J. Appl. Crystallogr. **30**, 171 (1997).

[26] Y. Tabira, R. L. Withers, T. Yamada, and N. Ishizawa, Z. Kristallogr. **216**, 92 (2001).

[27] I. D. Brown, *The Chemical Bond in Inorganic Chemistry: The Bond Valence Model*, IUCr Monographs in Crystallography (Oxford University Press, Oxford, 2002).

[28] I. D. Brown and D. Altermatt, Acta Crystallogr., Sect. B: Struct. Crystallogr. Cryst. Chem. **41**, 244 (1985).

[29] N. Metropolis, A. W. Rosenbluth, M. N. Rosenbluth, A. H. Teller, and E. Teller, J. Chem. Phys. **21**, 1087 (1953).